Geotextiles and Geomembranes 43 (2015) 547–557

Contents lists available at ScienceDirect

Geotextiles and Geomembranes

journal homepage: www.elsevier.com/locate/geotexmem

PVD improvement of soft Bangkok clay with and without vacuum preloading using analytical and numerical analyses

Le Gia Lam [a, c, *], Dennes T. Bergado [a, b, **], Takenori Hino [a]

[a] Institute of Lowland and Marine Research, Saga University, Honjo machi 1, Saga 840-8502, Japan
[b] Asian Institute of Technology, Pathumthani 12120, Thailand
[c] Can Tho University, Can Tho, Viet Nam

ARTICLE INFO

Article history:
Received 24 February 2015
Received in revised form
16 March 2015
Accepted 7 April 2015
Available online 14 August 2015

Keywords:
Vacuum PVD
Vacuum preloading
PVD improvement
Bangkok clay improvement
Embankment preloading

ABSTRACT

This paper presents the performance of improved soft Bangkok clay with prefabricated vertical drains (PVDs) combined with embankment preloading (conventional PVD method) and vacuum preloading (vacuum PVD method). The performance was evaluated in terms of settlements and flow parameters using analytical methods and numerical simulations in the ABAQUS software. The horizontal coefficient of consolidation (C_h), the ratio (k_h/k_s) between the horizontal hydraulic conductivity in the undisturbed zone (k_h) and the horizontal hydraulic conductivity in the smeared zone (k_s), and the final settlement (S_f) were back-calculated using the measured data. The sensitivity analysis was performed by varying the values of k_h/k_s. The vacuum PVD method was confirmed to have a higher rate of settlement than the conventional method. In particular, C_h increased from $4C_v$ to $5C_v$, k_h/k_s decreased from 8 to 7, and the consolidation time required to obtain a settlement of 1.30 m decreased from 300 days to 100 days. In addition, the calculated results from both the analytical method and FEM simulations for the conventional PVD agreed with the measured data. However, the results from the vacuum PVD method demonstrated that the FEM simulations yielded more reasonable results compared with the corresponding results obtained from the analytical methods.

1. Introduction

Soft grounds improved with prefabricated vertical drains (PVDs) combined with surcharge preloading is a popular technique used to accelerate the rate of consolidation and to shorten the construction time (Bergado et al., 1996a,b, 1999, 2002; Chai and Miura, 2000; Chai et al., 2001; Shen et al., 2005; Rowe and Taechakumthorn, 2008; Abuel-Naga et al., 2012; Ong et al., 2012; Deng et al., 2013; Cascone and Biondi, 2013; Bari and Shahin, 2014; Chung et al., 2014; Liu et al., 2014; Xue et al., 2014). PVDs are vertically installed into the soft ground after being preloaded by the embankment surcharge to generate a higher hydraulic gradient. This process causes the excess pore water to drain out of the soft clay towards the PVD and travel along the PVDs. However, this technique is limited by the embankment height and the instability of the embankment when embankment preloading to be increased in order to reduce the construction time. The vacuum consolidation was first applied by Kjellmann (1952) to reduce the consolidation period. Use of PVDs combined with embankment and vacuum preloading is an alternative method that solves the problems in conventional PVD. This process has been widely studied and applied (Holtz, 1975; Choa, 1989; Cognon et al., 1994; Bergado et al., 1998; Tang and Shang, 2000; Mohamedelhassan and Shang, 2002; Chu and Yan, 2005; Indraratna et al., 2004, 2005, 2009, 2010, 2012; Chai et al., 2003, 2005a,b, 2006a,b, 2007, 2008, 2010, 2013a; Xu and Chai, 2014; Bergado et al., 2006; Chu and Yan, 2006; Rujikiatkamjorn et al., 2007, 2008; Saowapakpiboon et al., 2008a,b, 2010a,b, 2011; Shahiduzzaman et al., 2010; Artidteang et al., 2011; Wu et al., 2013; Voottipruex et al., 2014; Lam et al., 2014). The advantage of this method is reducing the pore pressure, whereas maintaining a constant total stress instead of increasing the total stress as in conventional PVD. Thus, the effective stress is increased because of the reduction in the pore pressure assisted by the vacuum preloading. The net effect is an additional

* Corresponding author. Institute of Lowland and Marine Research, Saga University, Honjo machi 1, Saga 840-8502, Japan. Tel.: +81 952 28 8582; fax: +81 952 28 8189.
** Corresponding author. Asian Institute of Technology, Pathumthani 12120, Thailand. Tel.: +81 952 28 8582; fax: +81 952 28 8189.
E-mail addresses: lglam@ctu.edu.vn, legialam82@gmail.com (L.G. Lam), dbergado@gmail.com (D.T. Bergado).

http://dx.doi.org/10.1016/j.geotexmem.2015.07.013
0266-1144/

Table 1
Compressibility consolidation parameters.

Type	Unit weight [kN/m^3]	Compressibility			*POP* (kPa)	C_v_theory [m^2/year]
		RR	*CR*	C_α		
Top layer, weathered clay	18.50	0.035	0.350	0.014	45	–
Very soft clay1	13.80	0.050	0.500	0.020	37	0.79
Very soft clay2	14.00	0.042	0.420	0.017	59	0.79
Soft clay	15.00	0.040	0.400	0.016	100	0.79
Soft to medium clay	15.70	0.030	0.300	0.012	110	0.79
Stiff clay1	18.50	0.008	0.080	0.003	300	–
Stiff clay2	19.00	0.008	0.080	0.003	500	–
Stiff clay3	20.40	0.000	0.000	0.000	500	–

surcharge ensuring the early attainment of the required settlement and an increased shear strength resulting in increased embankment stability.

In practice, to maintain the vacuum pressure for the vacuum PVD is an engineering problem. Vacuum pressure is inevitably inconsistent because of the loss and supply during the consolidation process. Therefore, this study presents analytical methods and numerical simulations that consider the changes in vacuum preloading and embankment preloading. The soft Bangkok clay with the PVD combined with embankment preloading with and without vacuum preloading was applied at the Suvarnabhumi Bangkok International Airport Project (SBIA), Bangkok, Thailand; and the performance of this clay was investigated through the analytical analyses and numerical simulations compared with the measured data.

2. Site description and measurements

The data were monitored and collected at the Suvarnabhumi Bangkok International Airport Project (SBIA), Bangkok, Thailand. The soil profile and compressibility parameters at the SBIA are described in Table 1, in which *CC* is the compression ratio, *RR* is the recompression ratio, C_α is the coefficient of secondary compression, *POP* is the past overburden pressure, and C_v is the vertical coefficient of consolidation. The ground water was found at 5.0 m depth. The typical properties along with the soil parameters are summarized in Fig. 1 (Bergado et al., 2002). Both the conventional and vacuum techniques were applied at the site to improve the soft clay (Fig. 2), as reported by COFRA (1996).

For the conventional PVD method, the PVD type of MD 7007 was installed in square pattern with spacing of 1 m to the depth of 10 m. Characteristics of the PVD are summarized in Table 2. The soil was improved by preloading of embankment sand fill. The loading process comprised three stages. The first lift was 1.5 m height, the second lift was 2.8 m height and the third lift was up to 3.8 m height. The settlement was measured by using the surface settlement plate. The observed settlement was considered at locations SP-W5-021T and SP-W5-023T on the 3rd Runway Ked1 of SIBA. Construction process and measured settlement are plotted in Fig. 3.

For the vacuum PVD method, the PVD type of MD88H, which has a high resistance against lateral pressure, was installed to 10 m depth with a spacing of 0.85 m in a triangular pattern. The characteristics of the PVD are summarized in Table 2. The PVDs were connected via pressure equalization tubes (PE tubes) to the vacuum pump as shown in Fig. 4. The construction period, embankment lifts, vacuum preloading, and settlement were recorded at locations EW03-ZB01 and EW03-ZB05 as shown in Figs. 5 and 6, respectively.

3. Analytical calculations of settlements and flow parameters

The final settlements were calculated using the Asaoka (1978) observational method based on the monitored data from the field. The horizontal coefficient of consolidation, C_h, was also back-

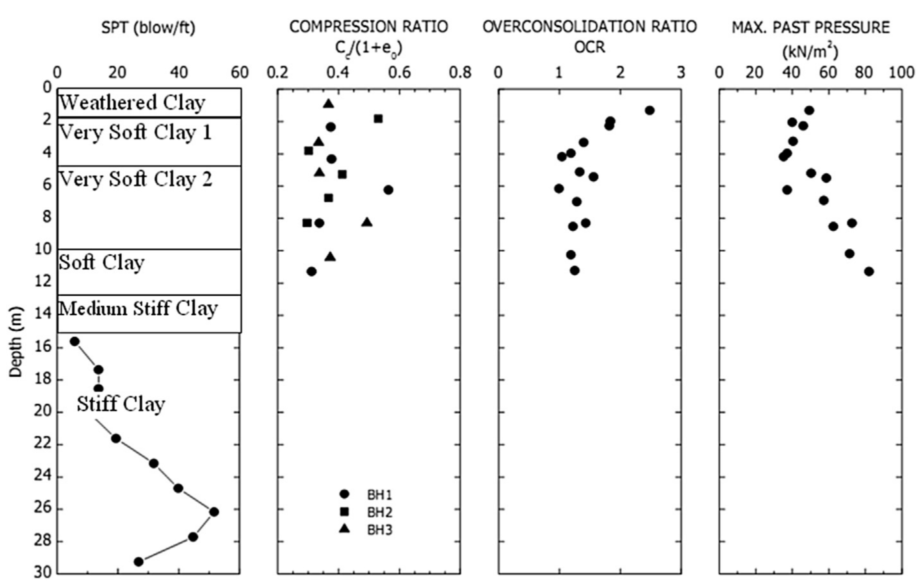

Fig. 1. Soil parameters of SBIA Project (Bergado et al., 2002).

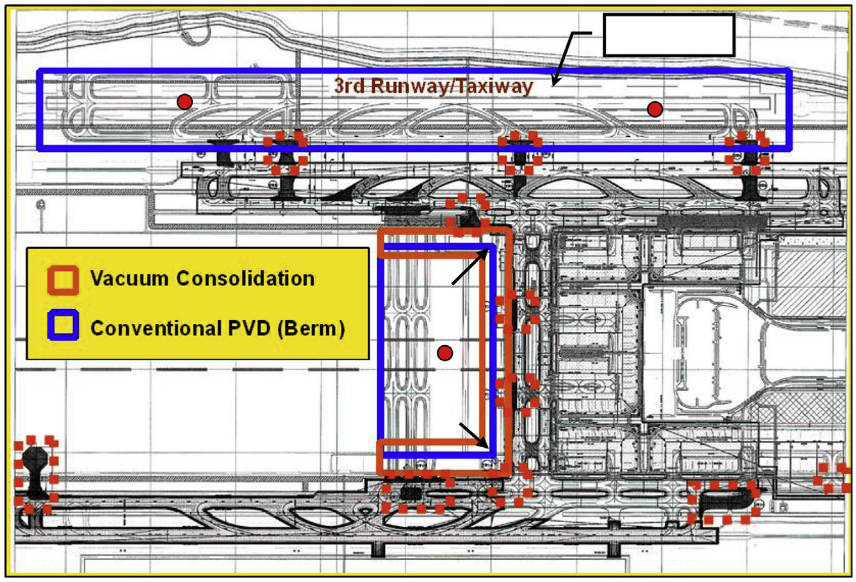

Fig. 2. The Midfield Satellite Aprons and Third Runway of Suvarnabhumi International Airport, Thailand showing the test areas.

calculated at different periods depending on the time of the installation of PVDs when the preloading period started.

The values of C_h were back-calculated using the equations from Hanbo (1979) for radial consolidation with PVD improvement:

$$U_h = \frac{S_t}{S_f} = 1 - \exp\left[\frac{-8T_h}{F}\right] \tag{1}$$

$$F = F(n) + F_s + F_r \tag{2}$$

where U_h is the degree of consolidation for horizontal drainage, S_t is the measured settlement at time t, S_f is the final settlement using the Asaoka's method (1978), T_h is the time factor for horizontal drainage, and F is factor of the PVD geometry. The values of $F(n)$, F_s and F_r are given by the following equations:

$$F(n) = \ln\left[\frac{D_e}{d_w}\right] - \frac{3}{4} \tag{3}$$

Table 2
Parameters related to conventional and vacuum PVDs.

Item	Conventional PVD	Vacuum PVD
PVD Type	MD 7007	MD 88
Pattern	Square	Triangular
Drain spacing, S (m)	1	0.85
Diameter of the equivalent soil cylinder, D_e (m)	1.13	0.8925
Cross section of PVD		
b_w (m)	0.10	0.10
t_w (m)	0.003	0.0035
Diameter of the equivalent drain, d_w (m)	0.0515	0.0518
Cross section of Mandrel		
w_m (m)	0.06	0.06
l_m (m)	0.12	0.12
Diameter of the equivalent mandrel, d_m (m)	0.0957	0.0957
Diameter of the equivalent smear zone, d_s (m)	0.1915	0.1915
Length of PVD, L (m)	10	10

$$F_s = \left[\frac{k_h}{k_s} - 1\right]\ln\left[\frac{d_s}{d_w}\right] \tag{4}$$

$$F_r = \frac{2}{3}\pi L^2 \frac{k_h}{q_w} \tag{5}$$

where D_e is the diameter of the equivalent soil cylinder, d_w is the equivalent diameter of the drain, k_h is the coefficient of horizontal permeability, k_s is the horizontal permeability of the smear zone, d_s is the diameter of the smear zone, L is designated as half the length of the PVD for double drainage and the full length of the drain for single drainage, and q_w is the discharge capacity of the drain at a hydraulic gradient of 1 (one). The diameter of the smear zone, d_s, is designated as twice the equivalent diameter of the mandrel, d_m. The discharge capacity, q_w, was designated as $A_w k_w$, where A_w and k_w are the cross-section and longitudinal permeability of the drain, respectively. The time factor, T_h, for horizontal drainage can be calculated using the following:

$$T_h = \frac{C_h t}{D_e^2} \tag{6}$$

where C_h is the coefficient of horizontal consolidation and t is the time elapsed after the application of the load.

Substituting Eqs. (2)–(6) into Eq. (1), the horizontal coefficient of consolidation, C_h, can be determined. As a result, the degree of consolidation is also calculated using Eq. (1). In addition, sensitivity analyses were performed by varying the values of C_h and k_h/k_s.

Because of the limited recorded data for the first phase preloading for the conventional PVD method, an analysis comprising only two phases was performed. The first phase combines the first and second stage loading, and the second phase corresponds to the third lift of the embankment. Fig. 7 shows the analyzed results at location SP-W5-021T. The back-analysis value of C_h was 1.655E-07 m^2/s, and the k_h/k_s was 8 during the first phase. The C_h decreased to 1.306E-07 m^2/s during the second phase. The final settlement, S_f, was 1.64 m. Similarly, the results at location SP-W5-023T are shown in Fig. 8, in which S_f was 1.60 m, k_h/k_s was 8, C_h during the combined first and second lifts was 1.690 m^2/s, and C_h during the third stage

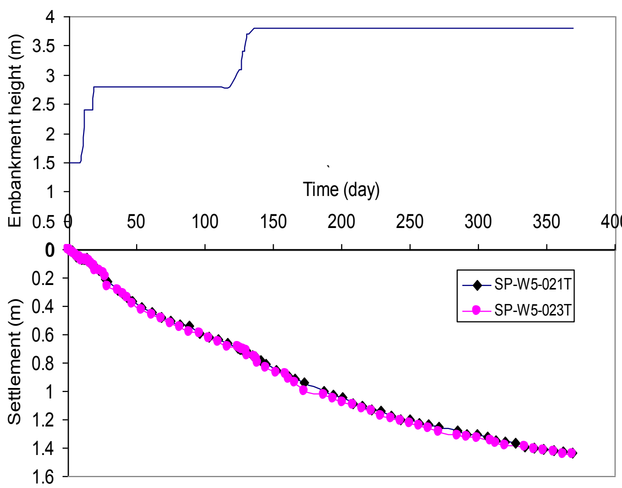

Fig. 3. Embankment loading and observed data for conventional PVD schemes.

loading was 1.402 m^2/s. At a consolidation time of 300 days, the settlements were 1.31 m and 1.34 m, corresponding to 80% and 84% degree of consolidation at locations SP-W5-021T and SP-W5-023T, respectively.

For the vacuum PVD, the calculated results at location EW03-ZB01 are shown in Fig. 9, in which the C_h was 1.744E-07 m^2/s, and k_h/k_s was 7, and S_f was 1.69 m. The C_h was 3.095E-07 m^2/s, and k_h/k_s was 7, and S_f was 1.39 m at location EW03-ZB05 as shown in Fig. 10. At a consolidation time of 100 days, the settlements were 1.23 m and 1.31 m corresponding to 73% and 92% degree of consolidation at the locations EW03-ZB01 and EW03-ZB05, respectively.

4. Numerical simulations

The FEM simulation of the improved zone using the equivalent vertical permeability, k_{ev}, was proposed by Chai et al. (2001). The equivalent vertical permeability, k_{ev}, was derived by converting the expressions of Carillo (1942) and Hansbo (1981) into an one-dimensional drainage. The equivalent vertical permeability is given as follows:

Fig. 4. Applied vacuum PVDs at SBIA.

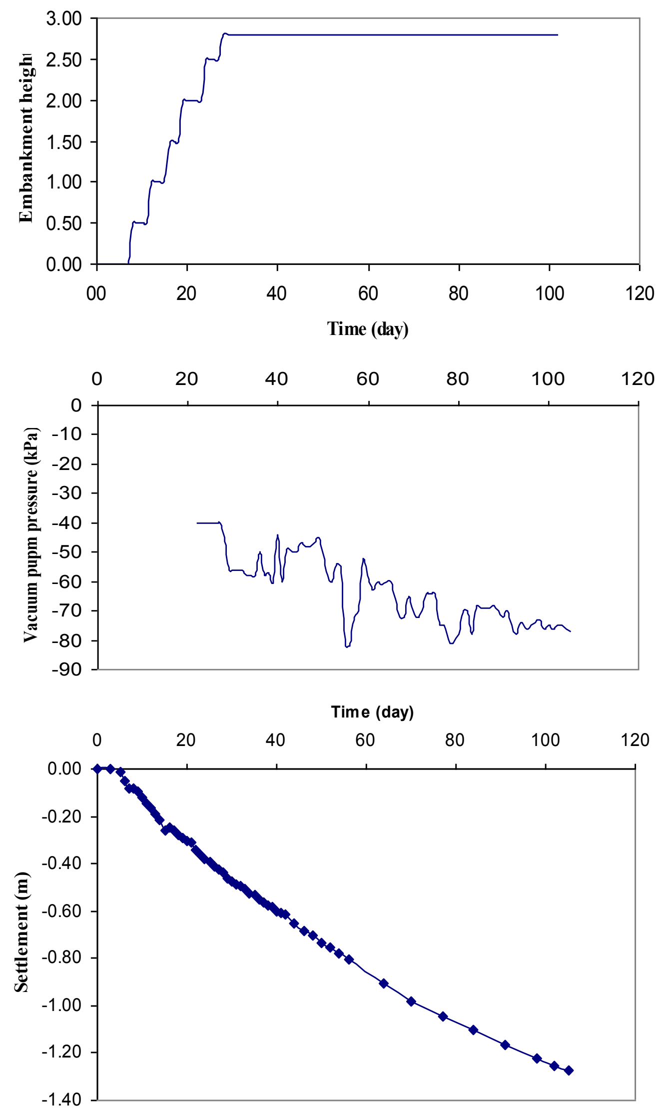

Fig. 5. Construction loading and observed measurement for vacuum PVD at location EW03-ZB01.

$$k_{ev} = \left(1 + \frac{2.5l^2}{\mu D_e^2}\frac{k_h}{k_v}\right)k_v \quad (8)$$

where:

k_h, k_v = permeability of undisturbed soil in the horizontal and vertical direction, respectively.
l = drainage length of the PVD improved zone.
μ = factor of the PVD geometry as expressed by Hansbo (1981).

$$\mu = \ln\left(\frac{n}{s}\right) + \frac{k_h}{k_s}\ln(s) - \frac{3}{4} + \frac{\pi 2l^2 k_h}{3q_w} \quad (9)$$

where the parameters have been defined previously.

ABAQUS software was applied to the axisymmetric FEM model based on the Biot consolidation theory to simulate the 2D drain (Hibbitt et al., 2006). Although a 3D model likely produces a more

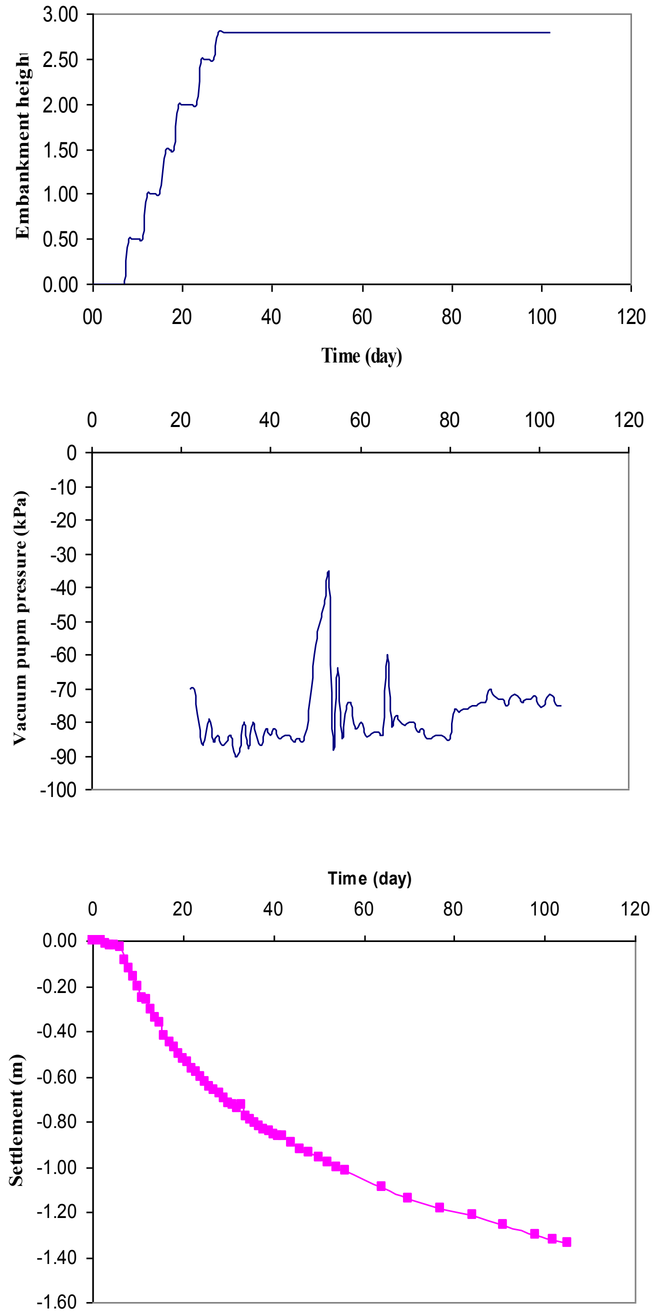

Fig. 6. Construction loading and observed measurement for vacuum PVD at location EW03-ZB05.

accurate result, Rujikiatkamjorn et al. (2008) and Indraratna et al. (2009) showed that the predicted results in a three-dimensional and two-dimensional multi-drain finite element analyses (ABAQUS) are similar. Moreover, Chai et al. (2013b) concluded that the k_{ev} method provides as good results as that of the explicitly modeling methods. Additionally, to simplify the model and shorten the analysis time, the 2D axisymmetric models were selected. The 2D axisymmetric mesh was employed to the equivalent permeability (k_{ev}) for the horizontal (k_h) permeability, vertical (k_v) permeability and dimensions of PVD as derived from Eq. (8). Through the input of a specific cross sectional area, A_w, and discharge capacity, q_w, or permeability of k_w for the drainage element, the well resistance can be introduced to the analysis. The

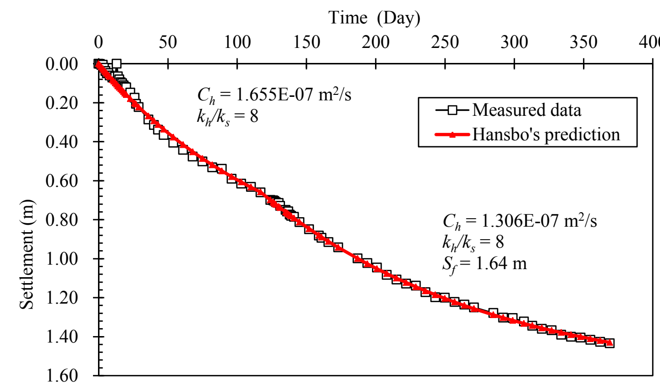

Fig. 7. Analytical results for conventional PVD at location SP-W5-021T.

simulation parameters are showed in Table 3. The horizontal permeability was assumed to be twice the vertical permeability. The Modified Cam Clay model and CAX8RP (8-node biquadratic displacement, bilinear pore pressure) element in a 2D plane strain were used in the simulations. Phase analyses were applied to correspond with the loading stages of the construction process.

For the conventional PVD schemes, the model using phase analyses is shown in Fig. 11. Three phases were analyzed corresponding to 1.5 m, 2.8 m and 3.5 m embankment height. The mechanism of the consolidation process in the phase analyses is illustrated in Fig. 12. The excess pore water pressure suddenly increased after the load was applied, and then gradually reduced

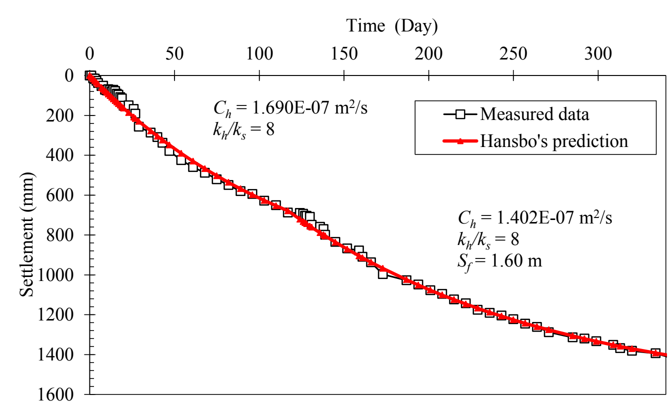

Fig. 8. Analytical results for conventional PVD at location SP-W5-023T.

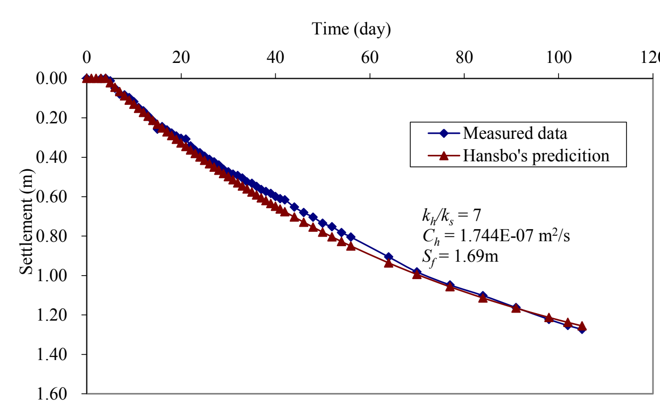

Fig. 9. Analytical results for vacuum PVD at location EW03-ZB01.

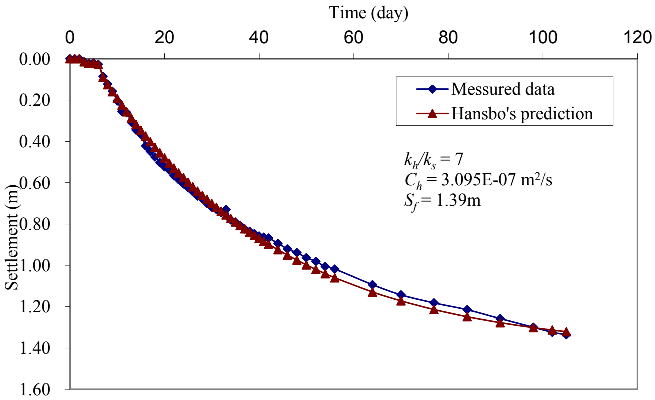

Fig. 10. Analytical results for vacuum PVD at location EW03-ZB05.

corresponding to the increase of settlement with elapsed time. For the vacuum PVD cases, phase analyses were applied to correspond to the construction loading of the embankment height and the recorded applied vacuum preloading. The FEM model is shown in Fig. 13.

Consequently, the sensitivity analyses to demonstrate the effects of the smeared zone on the consolidation rate were carried performed by varying the ratio of k_h/k_s as shown in Figs. 14 and 15 for the conventional PVD at locations SP-W5-021T and SP-W5-023T, respectively. At the two locations, the value of the ratio of k_h/k_s was 8, and the horizontal consolidation coefficient C_h was $5C_v$ during the first and second phases and $4C_v$ during the third phase. The final settlement, S_f, was 1.66 m as shown in Figs. 16 and 17. The value of C_v depends on the subsoil layers as demonstrated in Table 3. After 300 days of consolidation, the simulated settlement was 1.33 m corresponding to 80% degree of consolidation. For the vacuum PVD schemes, the effects of the smeared zone were illustrated through the sensitivity analyses as shown in Figs. 18 and 19 at locations EW03-ZB01 and EW03-ZB05, respectively. The value of C_h equaled $5C_v$, and k_h/k_s was 7 at both locations, EW03-ZB01 and EW03-ZB05, as shown in Figs. 20 and 21. The final settlements were 1.71 m and 1.43 m at locations EW03-ZB01 and EW03-ZB05, respectively. After a consolidation time of a hundred days, the settlements were 1.25 m and 1.31 m (corresponding to 73% and 90% degree of consolidation) at locations EW03-ZB01 and EW03-ZB05, respectively. The simulated values of C_v were 3.488E-08 m^2/s at the first subsoil layer, and 2.537E-08 m^2/s at the second and third subsoil layers in the PVD improved zone. In summary, the values of C_h at the improved zone ranged from 1.018E-07 to 1.738E-07 m^2/s, corresponding to a k_h/k_s of 8 for the conventional PVD; values of C_h are approximately 1.272E-07 to 1.738E-07 m^2/s, corresponding to a k_h/k_s of 7 for the vacuum PVD.

5. Discussions

Both the analytical and numerical methods provided results which well matched the measured data. For the analytical method, the results indicate that C_h was changed during the preloading process for the conventional PVD cases. In particular, C_h decreased from 1.655E-07 m^2/s and 1.690E-07 m^2/s during the combination of the first and second lifts to 1.306E-07 m^2/s and 1.402E-07 m^2/s during the third lift at locations SP-W05-021T and SP-W5-023T, respectively. Similar results were found in the numerical simulations. FEM results show a decrease in C_h from $5C_v$ during the first and second stage loading to $4C_v$ during the third stage loading at both locations SP-W05-021T and SP-W05-023T. Both the analytical and numerical results indicate a consistent value of ratio of the k_h/k_s equaling 8 for each stage of loading. This behavior results from the ground being pre-consolidated mainly in the vertical direction because of the first and second lifts. The values of analytically predicted S_f for locations SP-W5-21T and SP-W5-23T were slightly different as shown, respectively, in Figs. 7 and 8 because of the small difference between the observed settlements of the two locations as shown in Fig. 3. However, in both locations the same

Table 3
Simulation parameters of soft Bangkok clay.

Layer	H (m)	e_0	γ (kN/m^3)	k_v (m/s)	C_v (m^2/s)	κ	ν	λ	M	e_{cs}
1	2	1.35	18.5	8.125E-10	3.472E-08	0.036	0.3	0.357	0.9	2.11
2	3	2.52	13.8	5.845E-10	2.546E-08	0.076	0.3	0.764	0.9	4.90
3	5	2.44	14.0	5.845E-10	2.546E-08	0.063	0.3	0.627	0.95	4.73
4	3	11.8	15.0	9.745E-10	4.167E-08	0.049	0.3	0.486	1.1	3.76
5	2	1.46	15.7	9.745E-10	4.167E-08	0.032	0.3	0.321	1.1	2.86

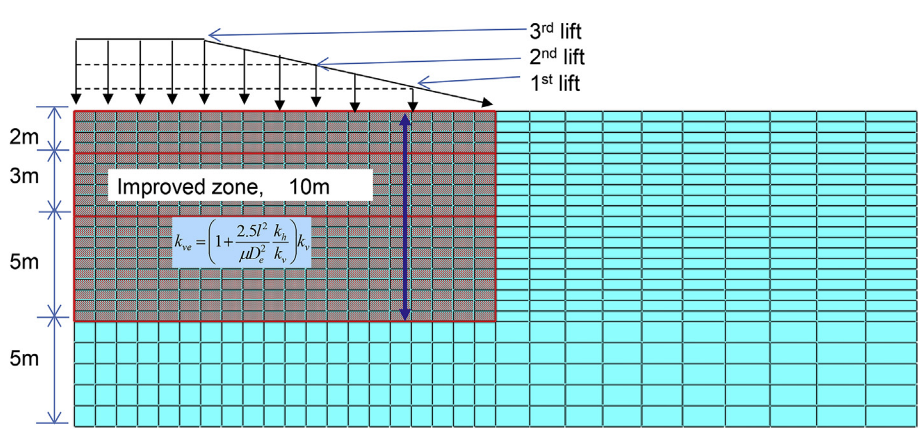

Fig. 11. FEM model for the conventional PVD.

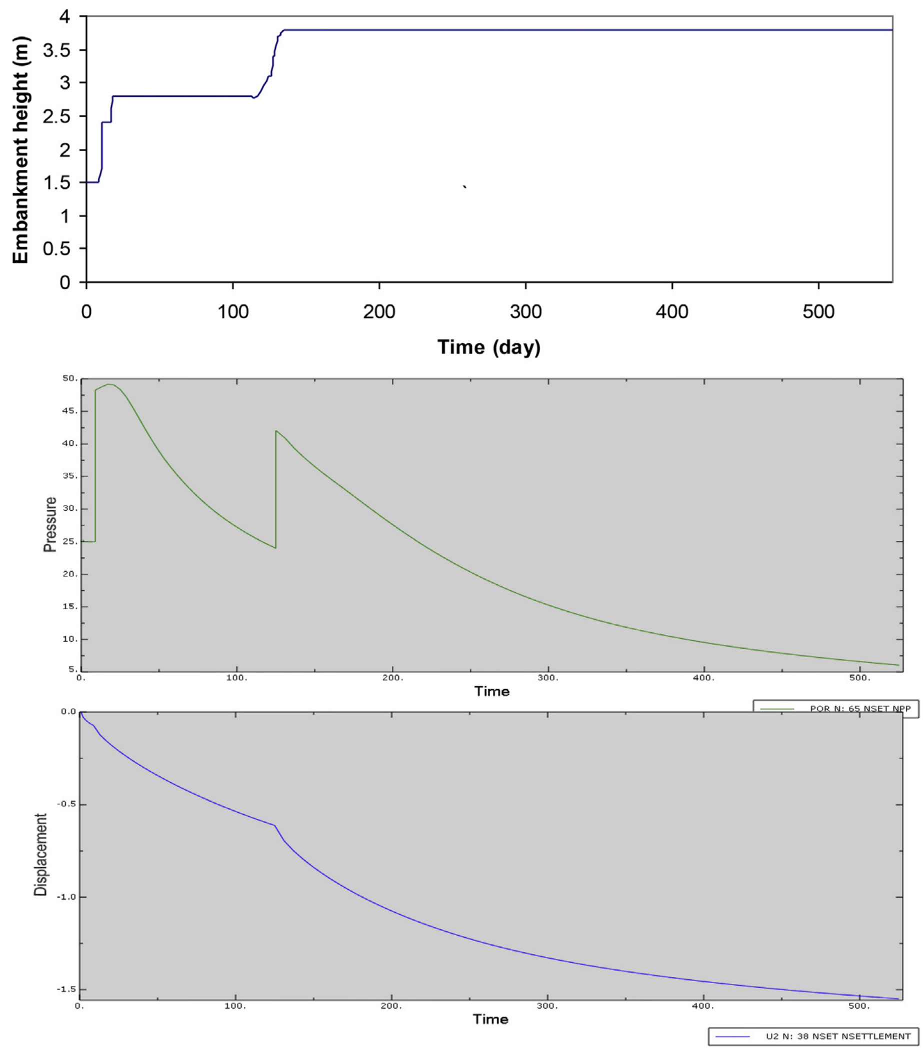

Fig. 12. Consolidation process for the conventional PVD.

procedure of embankment stage loading were applied as shown in Fig. 3, and numerically simulated using the same parameters as tabulated in Table 3 which resulted in the same S_f obtained from FEM simulations for the two locations as shown in Figs. 16 and 17. Both analytical methods and FEM simulations took into account the embankment stage loading using phase analyses. Thus, the resulting analytical and numerical values of S_f were slightly different but they agreed with the measured data as compared in Figs. 16 and 7 as well as in Figs. 17 and 8. In addition, the numerical sensitivity analyses imply that the effects of the smeared zone by the ratio of k_h/k_s dominate the consolidation process. Smaller values of k_h/k_s produce the faster consolidations will perform. Engineers and designers should be aware of this factor.

For the vacuum PVD, the results show that C_h generally increased and the ratio of k_h/k_s decreased when compared with the results from conventional PVD cases. However, the analytical

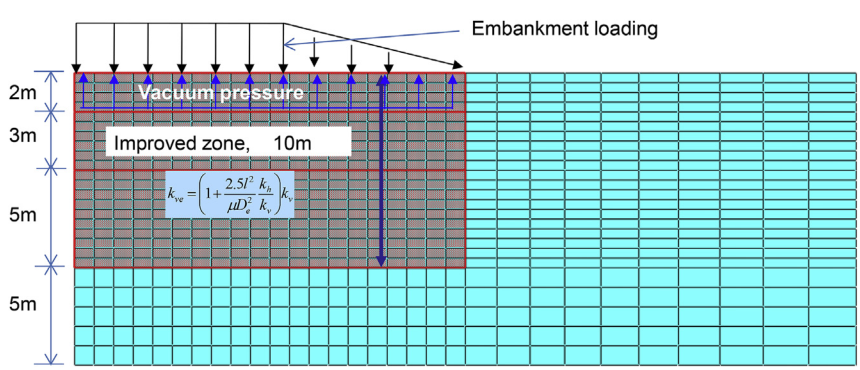

Fig. 13. FEM model for the vacuum PVD.

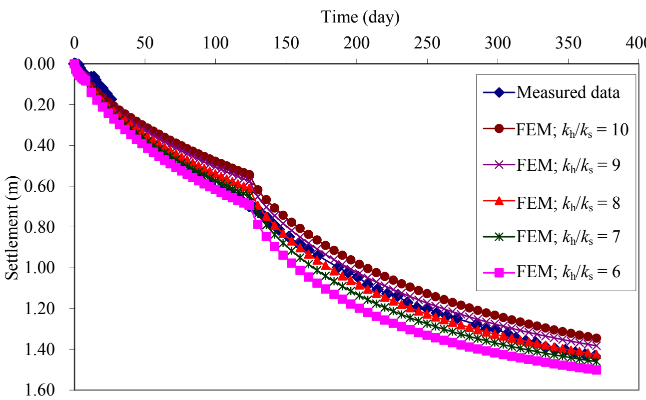

Fig. 14. Sensitivity analyses for conventional PVD at location SP-W5-021T.

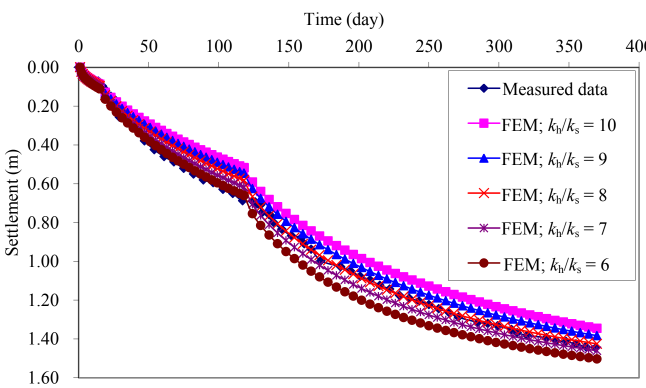

Fig. 15. Sensitivity analyses for conventional PVD at location SP-W5-023T.

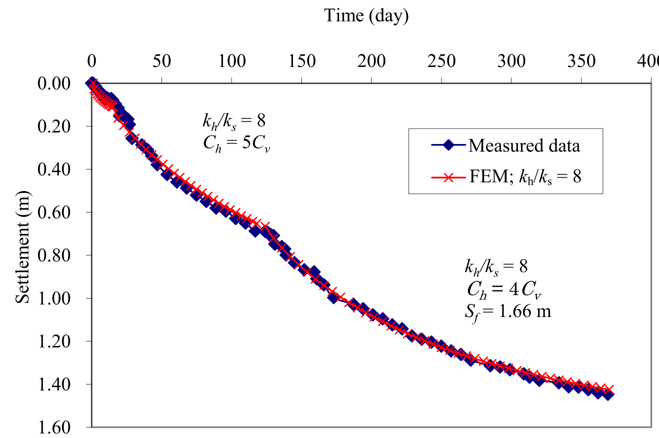

Fig. 17. FEM results for conventional PVD at location SP-W5-023T.

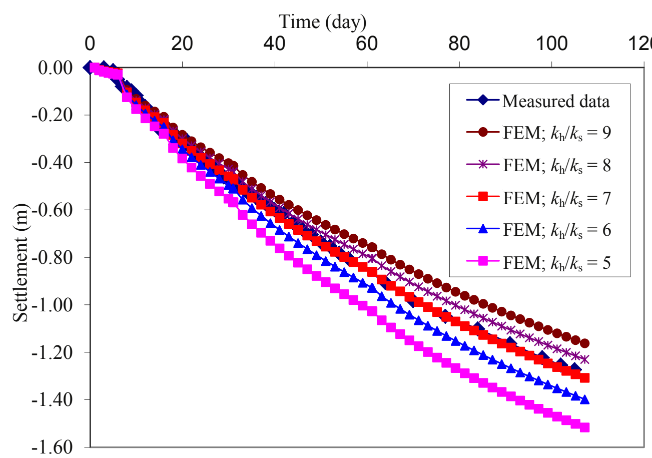

Fig. 18. Sensitivity analyses for vacuum PVD at location EW03-ZB01.

method shows that the value of C_h at location EW03-ZB05 is approximately twice that at location EW03-ZB01. The predicted final settlement of 1.39 m at location EW03-ZB05 is approximately 21% smaller than that of 1.69 m at location EW03-ZB01. The data showed that the consolidation rate accelerated with time at location EW03-ZB01 whereas slowed with time at location EW03-ZB05. This difference in behavior resulted from increasing with time at location EW03-ZB01 whereas reducing with time at location EW03-ZB05, as shown in Figs. 5 and 6. Fortunately, the FEM simulations considered changing vacuum pressures, therefore, the results were reasonable and well matched the measured values, as shown in Figs. 20 and 21. The FEM results revealed the identical value of C_h of 5C_v and k_h/k_s of 7 at the two locations. In addition, the FEM simulations found that the effective vacuum pressure (which was the actual vacuum pressure acting on the consolidation process) ranged from −36 kPa to −50 kPa and from −40 kPa to −65 kPa, corresponding to 72%–69% and 57%–76% of the vacuum

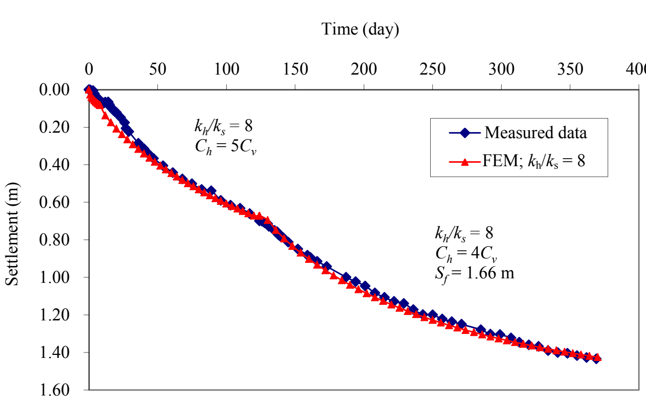

Fig. 16. FEM results for conventional PVD at location SP-W5-021T.

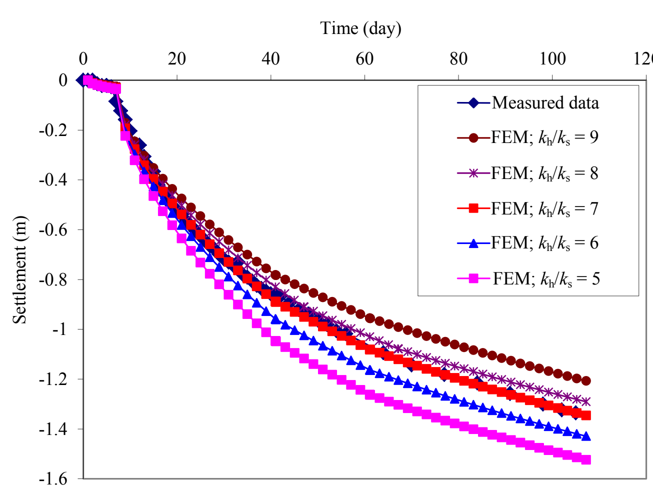

Fig. 19. Sensitivity analyses for vacuum PVD at location EW03-ZB05.

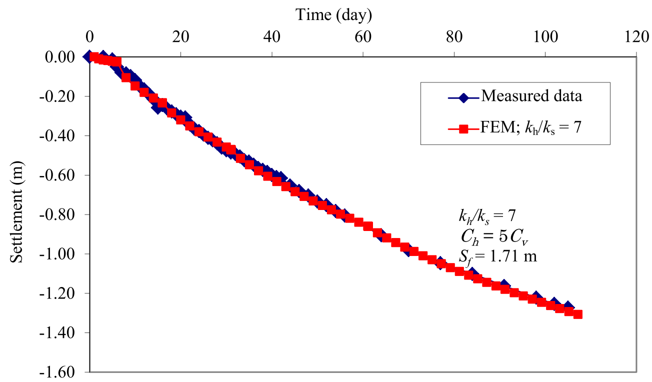

Fig. 20. FEM results for vacuum PVD at location EW03-ZB01.

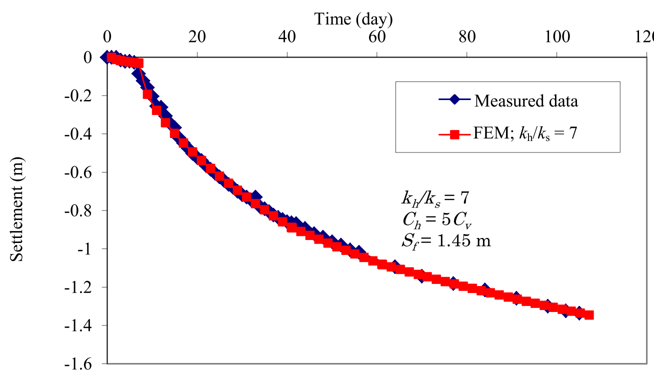

Fig. 21. FEM results for vacuum PVD at location EW03-ZB05.

pump pressure at locations EW03-ZB01 and EW03-ZB05, respectively. In other words, partial loss of vacuum pressure was noted during the consolidation process; this loss was as also demonstrated in the recorded data in Fig. 22. The vacuum pressure could be leaking at the connection between the tube and PVD. Moreover, the sensitivity analyses express that a smaller value of k_h/k_s results in a faster consolidation rate.

In summary, the calculated values of C_h from the vacuum PVD are correspondingly larger than that of the conventional PVD. Compared with the conventional PVD the ratio of k_h/k_s was reduced for the vacuum PVD, resulting from the effects of the vacuum pressure distribution with depth. The vacuum pressure maintained a constant effective vacuum pressure along the PVDs as demonstrated by Chai et al., 2010, in which the vacuum pressure applied with PVD distributes constantly along the drain in the condition of

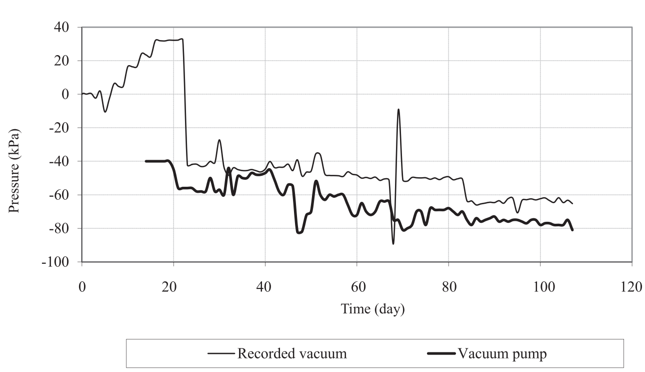

Fig. 22. Vacuum pump and recorded vacuum pressure at location EW03-ZB01.

without vacuum loss, whereas the effects of the embankment preloading significantly reduce with depth as controlled by the stress distribution. For the construction time, the vacuum PVD was more efficient than the conventional PVD. To obtain the expected settlement from 1.2 m to 1.4 m, the locations that applied the vacuum PVD required only 100 days, whereas the locations using the conventional PVD required 300 days. Therefore, the vacuum PVD not only solves the problem of stability of embankment slopes but also significantly reduces the consolidation time.

6. Conclusions

Based on the measured data and calculated results, the following conclusions can be drawn:

1. Both the analytical methods and numerical simulations indicate that the rate of consolidation for the vacuum PVD cases is faster than that of the conventional PVD cases schemes because of the increased coefficient of consolidation, C_h, and the reduced effects of the smeared zone corresponding with reductions in the ratio k_h/k_s.
2. To achieve a settlement of 1.30 m, 100 days and 300 days were required for the vacuum PVD and the conventional PVD, respectively.
3. For the conventional PVD only, the decrease of C_h values ($5C_v$–$4C_v$) refer to the second stage loading compared with the first loading.
4. The vacuum PVD showed that C_h increased from $4C_v/5C_v$ (referred to the second/first stage loading for the conventional PVD) to $5C_v$; the ratio k_h/k_s decreased from 8 to 7.
5. The effects of the smeared zone were investigated in terms of the k_h/k_s ratio in the sensitivity analyses. Reducing the k_h/k_s ratio results in increasing the consolidation rate.
6. The effective vacuum, which acted on the consolidation process, was approximately 57%–76% of the vacuum pump pressure.
7. Phase analyses refer to the embankment stage loading for the conventional PVD method as well as the changes of the vacuum pressures for the vacuum PVD method. The results agreed with the measured data for each stage loading.
8. FEM simulations produced better results than the analytical analyses when the preloading was not constant. Notably, when the vacuum changed, the FEM results at the two locations were more reasonable than those from the analytical calculations.

Acknowledgments

The authors would like to acknowledge the Royal Thai Government (RTG) and Maruyama Industry Co., Ltd. for their financial support in this research.

References

Abuel-Naga, H.M., Pender, M.J., Bergado, D.T., 2012. Design curves of prefabricated vertical drains including smear and transition zones effects. Geotext. Geomembr. 32 (1), 1–9.
Artidteang, S., Bergado, D.T., Saowapakpaiboon, J., Teerachaikulpanich, N., Kumar, A., 2011. Enhancement of efficiency of prefabricated vertical drain using surcharge, vacuum and heat preloading. Geosynth. Int. 18 (1), 35–47.
Asaoka, A., 1978. Observational procedure of settlement prediction. Soils Found. 18 (4), 87–101.
Bari, M.W., Shahin, M.A., 2014. Probabilistic design of ground improvement by vertical drains for soil of spatially variable coefficient of consolidation. Geotext. Geomembr. 42 (1), 1–14.
Bergado, D.T., Manivannan, R., Balasubramaniam, A.S., 1996a. Filtration criteria for prefabricated vertical drain geotextile filter jacket in soft Bangkok clay. Geosynth. Int. 3 (1), 63–83.
Bergado, D.T., Long, P.V., Balasubramaniam, A.S., 1996b. Compressibility and flow parameters from PVD improved soft Bangkok clay. Geotech. Eng. J. 27 (1), 1–20.

Bergado, D.T., Balasubramaniam, A.S., Chishti, I.A., 1999. Evaluation of the PVD performance at the Second Bangkok Chonburi Highway (SBCH) project. Lowl. Technol. Int. J. 1 (2), 55–75.
Bergado, D.T., Balasubramanian, A.S., Fannin, R.J., Holtz, R.D., 2002. Prefabricated vertical drain (PVD) in soft Bangkok clay: a case of NBIA project. Can. Geotech. J. 39, 304–315.
Bergado, D.T., Chai, J.C., Miura, N., Balasudramaniam, A.S., 1998. PVD improvement of soft Bangkok clay with combine vacuum and reduced sand embankment preloading. Geotech. Eng. J. 29 (1), 95–121.
Bergado, D.T., Sawapakpiboon, J., Korittayanon, N., De Zwart, T.P., 2006. Ceteau-S PVD vacuum system in soft Bangkok clay: a case study of the Suvarnablumi Airport Project. In: Proceedings 6th Symposium on Soft Ground Improvement and Geosynthetics Bangkok, Thailand, pp. 18–27.
Carillo, N., 1942. Simple two and three dimensional cases in the theory of consolidation of soils. J. Math. Phys. 21, 1–5.
Cascone, E., Biondi, G., 2013. A case study on soil settlements induced by preloading and vertical drains. Geotext. Geomembr. 38, 51–67.
Chai, J.C., Miura, N., 2000. A design method for soft subsoil improvement with prefabricated vertical drain. In: Proceedings of International Seminar on Geotechnics in Kochi, Japan, pp. 161–166.
Chai, J.C., Shen, S.L., Miura, N., Bergado, D.T., 2001. Simple method of modeling PVD improved subsoil. J. Geotech. Geoenviron. Eng. ASCE 127 (11), 965–972.
Chai, J.C., Miura, N., Nomura, T., Yoneya, H., 2003. Vacuum consolidation of soft clayey subsoil using cap-drain. In: Proceedings of the 18th Geosynthetics Symposium, Japan Branch, International Geosynthetics Society, vol. 18, pp. 231–236.
Chai, J.C., Carter, J.P., Hayahsi, S., 2005a. Ground deformation induced by vacuum consolidation. J. Geotech. Geoenviron. Eng. ASCE 131 (12), 1552–1561.
Chai, J.C., Hayashi, S., Carter, J.P., 2005b. Characteristics of vacuum consolidation. In: Proceedings of the 16th International Conference on Soil Mechanics and Geotechnical Engineering, International Society for Soil Mechanics and Geotechnical Engineering and the Japanese Geotechnical Society, Osaka, Japan.
Chai, J.C., Carter, J.P., Hayashi, S., 2006a. Vacuum consolidation and its combination with embankment loading. Can. Geotech. J. 43, 985–996.
Chai, J.C., Miura, N., Bergado, D.T., 2006b. Preloading clayey deposit by vacuum pressure with cap-drain. In: Proceedings of the 21st Geosynthetic Symposium, Aomori, Japan.
Chai, J.C., Miura, N., Nomura, T., 2007. Experimental investigated on optimum installation depth of PVD under vacuum consolidation. In: Proceedings of the 3rd China-Japan Joint Geotechnical Symposium, China.
Chai, J.C., Miura, N., Bergado, D.T., 2008. Preloading of clayey deposit by vacuum pressure with cap-drain: analyses versus performance. Geotext. Geomembr. 26 (3), 220–230.
Chai, J.C., Hong, Z.S., Shen, S.L., 2010. Vacuum-drain consolidation induced pressure distribution and ground deformation. Geotext. Geomembr. 28 (6), 525–535.
Chai, J.C., Ong, C.Y., Carter, J.P., Bergado, D.T., 2013a. Lateral displacement under combined vacuum pressure and embankment loading. Geotechnique 63 (10), 842–856.
Chai, J.C., Bergado, D.T., Shen, S.L., 2013b. Modelling prefabricated vertical drain improved ground in plane strain analysis. Ground Improv. 166 (G12), 65–77.
Choa, V., 1989. Drains and vacuum preloading pilot test. In: Proceedings 12th International Conference on Soil Mechanics and Foundation Engineering, Riode Janeiro. Brazil, pp. 1347–1350.
Chu, J., Yan, S.W., 2005. Estimation of degree of consolidation for vacuum preloading projects. Int. J. Geomech. 5, 158–165.
Chu, J., Yan, S.W., 2006. Effective depth of vacuum preloading. Lowl. Technol. Int. J. 8 (2), 1–8.
Chung, S.G., Kweon, H.J., Jang, W.Y., 2014. Observational method for field performance of prefabricated vertical drains. Geotext. Geomembr. 42 (4), 405–416.
COFRA (Thailand), 1996. Design and Proposal for the Execution of a Test Field: Vacuum Consolidation for the Landslide Road System for Second Bangkok International Airport, Bangkok, Thailand.
Cognon, J.M., Juran, I., Thevanayagam, S., 1994. Vacuum consolidation technology: principles and field experience. In: Proceedings Vertical and Horizontal Deformations of Embankments (Settlement'94). ASCE Special Publication, vol. 40 No.2, pp. 1237–1248.
Deng, Y.B., Xie, K.H., Lu, M.M., Tao, H.B., Liu, G.B., 2013. Consolidation by prefabricated vertical drains considering the time dependent well resistance. Geotext. Geomembr. 36, 20–26.
Hanbo, S., 1979. Consolidation of clay by band-shaped prefabricated drains. Ground Eng. 12 (5), 16–25.
Hansbo, S., 1981. Consolidation of fine-grained soils by prefabricated drains. In: Proceedings of the 10th International Conference on Soil Mechanics, Stockholm, vol. 3, pp. 677–682.
Hibbitt, Karlsson, Sorensen, 2006. ABAQUS/Standard User's Manual. HKS Inc.
Holtz, R.D., 1975. Preloading by vacuum: current prospects. Transp. Res. Rec. 548, 26–69.
Indraratna, B., Bamunawita, C., Khabbaz, H., 2004. Numerical modeling of vacuum preloading and field applications. Can. Geotech. J. 41, 1098–1110.
Indraratna, B., Rujikiatkamjorn, C., Sathananthan, L., 2005. Analytical and numerical solutions for a single vertical drain including the effects of vacuum preloading. Can. Geotech. J. 42, 994–1014.
Indraratna, B., Rujikiatkamjorn, C., Kelly, R., 2009. Modeling of combined vacuum and surcharge preloading with vertical drains. In: Proceedings of the 17th International Conference on Soil Mechanics and Geotechnical Engineering, Alexandria, Egypt, pp. 2204–2207.
Indraratna, B., Rujikiatkamjorn, C., Kelly, R., Buys, H., 2010. Sustainable soil improvement via vacuum preloading. Ground Improv. 163 (1), 31–42.
Indraratna, B., Rujikiatkamjorn, C., Balasubramaniam, A.S., McIntosh, G., 2012. Soft ground improvement via vertical drains and vacuum assisted preloading. Geotext. Geomembr. 30, 16–23.
Kjellmann, W., 1952. Consolidation of clay soil by means of atmospheric pressure. In: Proceedings on Soil Stabilization Conference, Boston, U.S.A, pp. 258–263.
Lam, L.G., Bergado, D.T., Voottipruex, P., Saowapakpiboon, J., Hino, T., 2014. Performance of PVDs improvement with and without vacuum preloading for soft ground. In: Proceedings of the 9th International Symposium on Lowland Technology, Japan, pp. 313–317.
Liu, J.C., Lei, G.H., Zheng, M.X., 2014. General solutions for consolidation of multilayered soil with a vertical drain system. Geotext. Geomembr. 42 (3), 267–276.
Mohamedelhassan, E., Shang, J.Q., 2002. Vacuum and surcharge combined one-dimensional consolidation of clay soils. Can. Geotech. J. 39 (5), 1126–1138.
Ong, C.Y., Chai, J.C., Hino, T., 2012. Degree of consolidation of clayed deposit with partially penetrating vertical drains. Geotext. Geomembr. 34, 19–27.
Rowe, R.K., Taechakumthorn, C., 2008. Combined effect of PVDs and reinforcement on embankments over rate-sensitive soils. Geotext. Geomembr. 26, 239–249.
Rujikiatkamjorn, C., Indraratna, B., Chu, J., 2007. Numerical modelling of soft soil stabilized by vertical drains, combining surcharge and vacuum preloading for a storage yard. Can. Geotech. J. 44 (3), 326–342.
Rujikiatkamjorn, C., Indraratna, B., Chu, J., 2008. 2D and 3D numerical modeling of combined surcharge and vacuum preloading with vertical drains. Int. J. Geomech. 8 (2), 144–156.
Saowapakpiboon, J., Bergado, D.T., Chai, J.C., Kovittayanon, N., De Zwart, T.P., 2008a. Vacuum-PVD combination with embankment loading consolidation in soft Bangkok clay: a case study of the Suvarnabhumi Airport Project. In: Proceedings of the 4th Asian Regional Conference on Geosynthetics, Shanghai, China, pp. 18–27.
Saowapakpiboon, J., Bergado, D.T., Hayashi, S., Chai, J.C., Kovittayanon, N., De Zwart, T.P., 2008b. CeTeau PVD vacuum system in soft Bangkok clay: a case study of the Suvarnabhumi Airport Project. Lowl. Technol. Int. 10 (1), 42–53.
Saowapakpiboon, J., Bergado, D.T., Artidteang, S., 2010a. Comparison on the performance of prefabricated vertical drain (PVD) preloading combined with and without vacuum and heat. Lowl. Technol. Int. J. 13 (1), 2–9.
Saowapakpiboon, J., Bergado, D.T., Youwai, S., Chai, J.C., Wanthong, P., Voottipruex, P., 2010b. Measured and predicted performance of prefabricated vertical drains (PVDs) with and without vacuum preloading. Geotext. Geomembr. 28 (1), 1–11.
Saowapakpiboon, J., Bergado, D.T., Voottipruex, P., Lam, L.G., Nakakuma, K., 2011. PVD improvement combined with surcharge and vacuum preloading including simulations. Geotext. Geomembr. 29 (1), 74–82.
Shahiduzzaman, M., Tanabashi, Y., Kawabata, H., Jiang, Y., Sugimoto, S., 2010. Reasonable management index in fill loading with vacuum consolidation method based on FEM analyses. Lowl. Technol. Int. J. 12 (2), 23–33.
Shen, S.L., Chai, J.C., Hong, Z.C., Cai, F.X., 2005. Analysis of field performance of embankments on soft clay deposit with and without PVD-improvement. Geotext. Geomembr. 23 (6), 463–485.
Tang, M., Shang, J.Q., 2000. Vacuum preloading consolidation of Yaogiang Airport runway. Geotechnique 50 (6), 613–653.
Voottipruex, P., Bergado, D.T., Lam, L.G., Hino, T., 2014. Back-analyses of flow parameters of PVD improved soft Bangkok clay with and without vacuum preloading from settlement data and numerical simulations. Geotext. Geomembr. 42 (5), 457–467.
Wu, Y.J., Yuan, Y.C., Chai, J.C., 2013. Performance of vacuum consolidation in a thick clayey deposit in Shanghai. Lowl. Technol. Int. J. 15 (2), 23–30.
Xu, F., Chai, J.C., 2014. Lateral displacement of PVD-improved deposit embankment loading. Geosynth. Int. 21 (5), 286–300.
Xue, J.F., Chen, J.F., Shi, Z.M., 2014. Instability of a geogrid reinforced soil wall on thick soft Shanghai clay with prefabricated vertical drains: a case study. Geotext. Geomembr. 42 (4), 302–311.

List of notations

A_w: the cross-section of the drain
b_w: width of the PVD
C_h: coefficient of consolidation in horizontal direction
C_v: coefficient of consolidation in vertical direction
CC: compression ratio
C_α: coefficient of secondary compression
POP: past overburden pressure
d_m: equivalent diameter of the mandrel
d_s: diameter of the smear zone
d_w: the equivalent diameter of the drain
D_e: diameter of the equivalent soil cylinder
e_0: initial void ratio of undisturbed soil
e_{cs}: void ratio at the critical state
F: factor of the PVD geometry
$F_{(n)}$: factor of spacing ratio
F_r: factor of well resistance

F_s: factor of smear effect
H: thickness of soil layer
k_{eq}: equivalent hydraulic conductivity
k_h: hydraulic conductivity of undisturbed soil in horizontal direction
k_v: hydraulic conductivity of undisturbed soil in vertical direction
k_s: hydraulic conductivity of disturbed soil in horizontal direction
k_w: longitudinal permeability of the drain
l: drainage length of the PVD improved zone
L: length of drainage path
l_m: length of the mandrel
M: slope of the critical sate line in the Modified Cam Clay
n: spacing ratio
q_w: discharge capacity of the drain at a hydraulic gradient of 1
RR: recompression ratio
s: smear ratio
S: Drain spacing
S_f: final settlement estimated by Asaoka's method or FEM
S_t: measured settlement time t
t: time elapsed after the application of the load
t_w: thickness of the PVD
T_h: time factor for horizontal drainage
U_h: degree of consolidation for horizontal drainage
w_m: width of the mandrel
κ: slope of the swelling line in the Modified Cam Clay
λ: slope of the normal line in the Modified Cam Clay
μ: factor of the PVD geometry
ν: specific volume in the Modified Cam Clay